

36. QUATERNARY MARINE AND CONTINENTAL PALEOENVIRONMENTS IN THE WESTERN MEDITERRANEAN (SITE 976, ALBORAN SEA): PALYNOLOGICAL EVIDENCE¹

Nathalie Combourieu Nebout,² Laurent Londeix,³ François Baudin,² Jean-Louis Turon,³ Rita von Grafenstein,⁴ and Rainer Zahn⁵

ABSTRACT

A continuous record of both marine and continental paleoenvironments in the Western Mediterranean has been investigated on the same samples from the composite core of Ocean Drilling Project (ODP) Leg 161, Site 976. Palynological analyses (pollen, dinoflagellate cysts, and organic matter) document the continental and marine paleoenvironmental changes in the Alboran Sea Basin from the beginning of the Pleistocene to the Holocene. The marine and continental records have been correlated to climate and/or hydrological changes.

The pollen record depicts the vegetation changes in southern Spain and in North Africa along the Pleistocene and Holocene. Variability in abundant and diversified dinoflagellate cyst assemblages permits us to identify climatic and hydrological variations of surface waters along the whole sequence. During the upper Pleistocene, eight climatic cycles are evidenced both in marine and continental paleoenvironments and correlated to the $\delta^{18}\text{O}$ curve. Focus on the last 28 calendar ka (cal ka) exhibits the major climatic events of the last climatic cycle: Last Glacial Maximum, Oldest Dryas, Bölling/Alleröd, Younger Dryas, and Holocene. Periods of enhanced productivity are evidenced between 19 and 17 cal ka and during the Younger Dryas.

INTRODUCTION

The Alboran Sea is a key location for understanding the influence of the Atlantic-Mediterranean gateways on Mediterranean paleoceanography. During Leg 161 of the Ocean Drilling Program (ODP), the *JOIDES Resolution* reoccupied the area of the Deep Sea Drilling Project (DSDP) Site 121 (Ryan, Hsü et al., 1973), located in the western Alboran Sea Basin (Fig. 1). As a palynological study was made on the long sequence recovered at DSDP Site 121, ODP Leg 161 Site 976 (36°12N, 4°18W) also allowed a good opportunity to obtain a continuous palynological record of the whole Pleistocene and improve our understanding of Atlantic/Mediterranean exchanges during this period.

The palynological study has been performed to allow direct land/sea correlations and simultaneously to show the modifications of western Mediterranean vegetation and the variations of Alboran Sea surface waters (in relation to entering Atlantic water) throughout the whole Pleistocene. Results are compared with the bulk gradient data of organic matter. The major continental and marine events have been linked to global climate and hydrological changes.

ENVIRONMENTAL SETTING

The Mediterranean area is divided in two main basins separated by the Siculo-Tunisian sill. Site 976 (Fig. 1) is located in the Alboran Sea, which represents the westernmost part of the Mediterranean, bordered in the north by Spain and in the south by Morocco. In the west, the Gibraltar Strait connects the Alboran Sea to the Atlantic

Ocean and allows watermass exchanges between Atlantic and Mediterranean waters, which partly balances the negative water budget of the Mediterranean Sea (e.g., Béthoux, 1979). The modern Alboran Sea hydrology is marked by an antiestuarine circulation (e.g., Lacombe and Tchernia, 1972). Surface waters from the Atlantic waters flow from the west to the east in the Alboran Sea in a wide anticyclonic gyre before moving toward the western and eastern Mediterranean basins. As a result, the Mediterranean intermediate and deep saline waters leave the Mediterranean Sea from the east to the west through the Gibraltar strait (e.g., Béthoux and Prieur, 1984; Fig. 1).

The present-day climate in the Alboran Sea region is Mediterranean with long, dry summers and mild winters. Aridity is highest along the southern Spanish coast, but peaks of precipitation occur in the Spanish hinterlands during spring and autumn. In northern Africa, rainfall is concentrated near the coast from autumn to spring, and it decreases strongly southward (Walter et al., 1975). In both areas, the Atlantic influence is marked by increasing humidity in the west. The presence of mountains (Moroccan Rif and Betic Cordillera) causes both humidity to increase and temperature to decrease with altitude. These landscapes display an altitudinal range of vegetation, according to the ecologic and climatic requirements of the plants, in the Moroccan Rif and in the Betic Cordillera (Ozenda, 1975; Rivas Martinéz, 1982; Barbero et al., 1981; Benabib, 1982). From the coast to the highest elevations, a steppe vegetation with *Lygeum*, *Artemisia* and/or a Mediterranean association (*Olea*, *Pistacia*, *Quercus ilex*) is first replaced by a deciduous *Quercus* forest and then by a coniferous forest with *Pinus*, *Abies*, and/or *Cedrus*. The latter lives only in Morocco today.

MATERIAL AND METHODS

Two hundred twenty-six samples were chosen for this study from Holes 976B, 976C, and 976D. According to the initial biostratigraphic framework (Comas, Zahn, Klaus, et al., 1996), our samples (up to 366 mcd [meters composite depth]) are representative of almost the whole Pleistocene and the Holocene. The uppermost 10 m span the last climatic cycle and have been sampled with a higher resolution (40 samples, ~0.25 m spaced). Underlying sediments have been studied with irregular spacing.

¹Zahn, R., Comas, M.C., and Klaus, A. (Eds.), 1999. *Proc. ODP, Sci. Results*, 161: College Station, TX (Ocean Drilling Program).

²ESA 7073 CNRS "Paléontologie et Stratigraphie," Université Pierre et Marie Curie (Paris VI), case courrier 116-117, 4 Place Jussieu, 75252 Paris cedex 05, France. nebout@ccr.jussieu.fr

³URA 197, Département de Géologie et Océanographie, Université Bordeaux I, Avenue des facultés, 33405 Talence cedex, France.

⁴Ludwig-Maximilian-University, Munich, Federal Republic of Germany.

⁵GEOMAR Research Center for marine Geosciences, Wischhofstrasse 1-3, 24148 Kiel, Federal Republic of Germany.

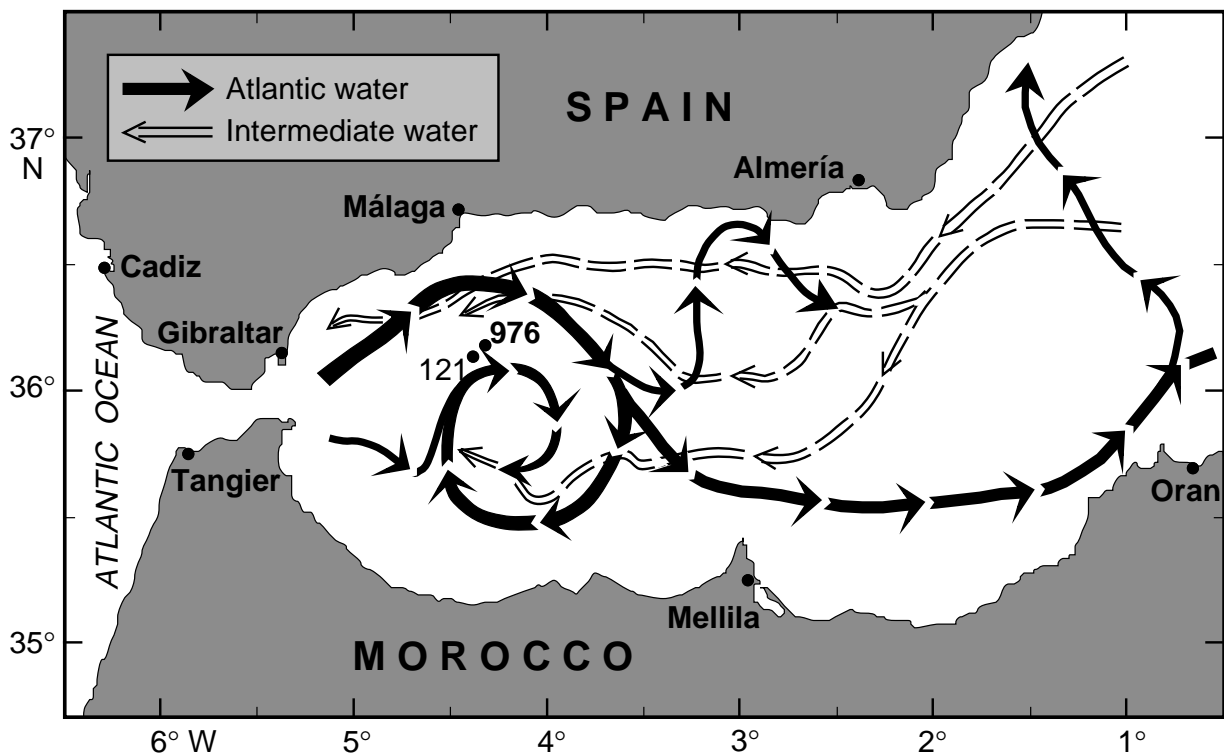


Figure 1. Present-day surface and intermediate water circulation in the Alboran Sea and location of Site 976.

After being dried and weighed, the samples were processed with 10% HCl, 70% HF, then 20% HCl, and sifted on a 10- μ m sieve. Each acid treatment was followed by neutralization with distilled water. Aliquot volumes of a calibrated *Eucalyptus* pollen suspension were added to each sample before chemical treatment in order to calculate palynomorph concentrations.

Pollen and dinoflagellate cysts were counted on the same slides. Pollen and dinocyst sums reached respectively at least 100 pollen grains, *Pinus* grains excluded, and at least 100 cysts, *Lingulodinium machaerophorum* excluded, in each sample.

Dinoflagellate cyst concentrations have been calculated on the total sum of dinocysts, including species that are sometimes heterotrophic, such as *Brigantedinium* spp. For now, palynomorph concentrations are presented only for the uppermost ten meters.

The productivity, the ease of transport, and good preservation of *Pinus* pollen grains often result in their over-representation in marine sediments (Brooks, 1971; Shaw, 1971; Duplessy et al., 1981; Rosignol and Planchais, 1989), which introduces discrepancies in the pollen diagram and tends to mask the variations of the other taxa and, consequently, the climate of the source area. For this reason, pollen percentages, except for *Pinus*, have been calculated on a sum that excludes this taxon. *Pinus* percentages are calculated on the total pollen sum.

Lingulodinium machaerophorum specimens are very abundant and frequently reach percentages above 40%. In order to emphasize significant but not abundant species, dinocyst percentages have been calculated on a sum that excludes *L. machaerophorum*. *L. machaerophorum* percentages are calculated on the total dinocyst sum. It is noteworthy that *L. machaerophorum* cysts in deep marine sediment can be doubtfully considered as autochthonous because of its fairly neritic modern distribution (Andreieff et al., 1971; Reid, 1977; Morzadec-Kerfourn, 1977; Wall et al., 1977; Bradford and Wall,

1984; Kobayashi et al., 1986; Matsuoka, 1985; Edwards and Andrieu, 1992; Mudie and Harland, 1996).

Following the Versteegh (1994) attempt, the ratio of most thermophile dinoflagellate cyst taxa vs. less thermophile ones (W/C) is used as a proxy for changes in sea-surface temperatures. In the present study, *Spiniferites mirabilis* s.l. (= *S. mirabilis* + *S. hyperacanthus*), *Selenopemphix nephroides*, *Impagidinium patulum*, *Impagidinium striatum*, *Operculodinium israelianum*, *Spiniferites delicatus*, and *Spiniferites membranaceus* are used as warm-water indicator species. On the opposite, *Nematosphaeropsis labyrinthica*, *Bitectatodinium tepikiense*, *Spiniferites elongatus*, *Impagidinium pallidum*, *Pentapleurosphaeridium* cf. *dalei* and *Algasphaeridium*? cf. *minutum* are used as cold-water indicators (Wall et al., 1977; Turon, 1984; Turon and Londeix, 1988; Edwards and Andrieu, 1992; de Vernal et al., 1994). *Operculodinium centrocarpum* is here considered to be a species too ubiquitous (e.g., Edwards and Andrieu, 1992; Mudie, 1992; de Vernal et al., 1994) to be used in such a ratio. The W/C value represents the number of cysts of warm-water indicator taxa (nW) vs. the number of cysts of cool-water indicator taxa (nC) plus nW.

All the samples taken at Site 976 have been analyzed for dinocysts. Because of the paucity of pollen grains, only 80 samples have presently been analyzed for pollen.

The amorphous organic matter (AOM) has been quantified in the palynological slides after a count of 200 organic particles and represented in terms of concentration calculated in the same way as the pollen and dinocyst concentrations. The AOM concentration curve is presented only for the uppermost 10 m.

Determination of total organic carbon in sediments is normally performed by subtraction of inorganic carbon from total carbon. In sedimentary rocks, virtually all inorganic carbon is confined to carbonate minerals. Therefore, we decide to include the carbonate carbon analysis as part of this study. Inorganic carbon content was de-

terminated by use of the carbonate bomb. Dried and weighed samples of exactly 100 mg were reacted in 2N HCl solution in a sealed bomb. Evolved carbon dioxide was measured by the mean of a manometer. The percentage of carbonate was calculated from the inorganic carbon (IC) content, assuming that all the carbonate was in form of calcite:

$$\text{CaCO}_3 = \text{IC} \cdot 8.332.$$

Total carbon (TC) content was determined using a LECO WR-12 analyzer. With this technique, organic and inorganic carbon were converted to carbon dioxide, which is measured with a thermal conductivity detector. Total organic carbon (TOC in wt%) content was calculated by difference between total carbon and carbonate carbon, according to the formula:

$$\text{TOC}\% = \text{TC}\% - \text{IC}\%.$$

The relative precision of TOC determination is defined by the combined precision of the TC and IC methods and is generally not better than 2%. These measurements have been performed up to 270 mcd.

The source of the organic matter were estimated using an Oil Show Analyser instrument (Espitalié et al., 1985a, 1985b, 1986) on the uppermost 10 mcd. Standard notations are used: S2 is in mg hydrocarbons (HC) per g of dry sediment and the hydrogen index (HI = S2/TOC·100) is expressed in mg HC/g TOC. The data are reported in Table 1.

The oxygen isotopic curve is from von Grafenstein et al. (Chap. 37, this volume). An initial time scale for Site 976 was developed by using biostratigraphic marker events of de Kaenel et al. (Chap. 13, this volume) and standard oxygen isotope stratigraphy (Imbrie et al., 1984; Ruddiman et al., 1989; Hodell and Venz, 1992; Sarnthein et al., 1995). The time scale was then refined by fitting the planktonic isotope record of Site 976 to the benthic oxygen isotope record from Site 659 in the subtropical Northeast Atlantic (Tiedemann et al., 1994). The Site 659 isotope record has been tuned to the obliquity component of the Earth's orbital elements and, thus, the time scale for Site 976 that is used here is considered an orbital time scale (for details of age-model development for Site 976 see von Grafenstein et al., Chap. 37, this volume). The ages given in this paper are presented in calendar ka (cal ka) according to the model developed by von Grafenstein et al. (Chap. 37, this volume).

RESULTS AND DISCUSSION

Marine Environment

All the samples studied are rich in dinocysts. On the whole, 55 dinoflagellate cyst taxa have been identified. Relative frequencies of these taxa show the succession of several types of associations, which are indicative of paleoclimatic and superficial paleohydrologic variations. However, dinocyst assemblages are nearly always dominated by *Brigantedinium* spp. (Fig. 2). *Nematosphaeropsis labyrinthea*, *Bitectatodinium tepikiense*, and *Spiniferites mirabilis* s.l. appear to be the other more significant species.

Former studies show that in Mediterranean Sea *Brigantedinium* spp. is not indicative of enhanced productivity (Turon and Londeix, 1988; Combourieu Nebout et al., 1998), by contrast with upwelling environments (Lewis et al., 1990; Biebow, 1996). Today, *N. labyrinthea* is an oceanic species encountered in cold to tropical environments (Harland, 1983; Rochon, 1997) and its optimal development coincides with high salinity environments and/or high nutrient avail-

Table 1. Results of carbonate and carbon analysis and Rock-Eval pyrolysis data of the uppermost 10 mcd of Site 976.

Core, section, interval (cm)	Depth (mcd)	CaCO ₃ (%)	TOC (%)	HI (mg HC/g TOC)
161-976C-				
1H-1, 5-7	0.06	19.3	0.46	111
1H-1, 29-31	0.30	22.0	0.46	122
1H-1, 54-56	0.55	22.9	0.12	111
1H-1, 78-80	0.79	27.2	0.45	106
1H-1, 104-106	1.05	24.2	0.37	100
1H-1, 129-131	1.30	23.7	0.63	145
1H-2, 4-6	1.55	23.9	0.52	128
1H-2, 27-29	1.78	24.7	0.44	116
1H-2, 54-56	2.05	27.9	0.54	97
1H-2, 78-80	2.29	26.7	0.89	180
1H-2, 104-106	2.55	28.7	0.55	150
1H-2, 129-131	2.80	27.2	0.92	142
1H-2, 146-148	2.97	27.7	0.69	156
1H-3, 4-6	3.05	24.7	0.42	106
1H-3, 27-29	3.28	23.7	0.58	133
1H-3, 51-53	3.52	24.8	0.77	150
1H-3, 78-80	3.79	27.0	0.81	175
1H-3, 99-101	4.00	24.2	1.47	172
1H-3, 129-131	4.30	27.3	0.96	209
1H-4, 2-4	4.53	26.3	0.93	127
1H-4, 29-31	4.80	25.2	0.75	116
1H-4, 51-53	5.02	22.3	1.02	131
1H-4, 78-80	5.29	18.6	1.05	68
1H-4, 104-106	5.55	18.1	1.40	85
1H-4, 126-128	5.77	19.7	1.50	89
161-976D-				
2H-4, 4-6	6.05	21.7	0.60	140
2H-4, 29-31	6.30	20.2	0.61	130
2H-4, 54-56	6.55	22.7	0.60	132
2H-4, 79-81	6.80	24.3	0.80	105
2H-4, 104-106	7.05	24.9	0.65	116
2H-5, 4-6	7.55	23.2	0.62	105
2H-5, 29-31	7.80	22.7	0.49	135
2H-5, 54-56	8.05	23.7	0.64	119
2H-5, 79-81	8.30	20.2	0.56	117
2H-5, 104-106	8.55	21.2	0.67	73
2H-5, 129-131	8.80	20.8	0.72	117
2H-6, 4-6	9.05	19.7	0.66	121
2H-6, 29-31	9.30	20.8	0.69	138
2H-6, 54-56	9.55	21.6	0.54	119
2H-6, 79-81	9.80	20.2	0.59	109
2H-6, 104-106	10.05	20.7	0.94	95
2H-6, 140-142	10.41	17.1	1.23	106

Note: Determination of the Total Organic Carbon (TOC) and the units of the various Rock-Eval parameters are given in the "Material and Methods" section.

ability (Wall and Warren, 1969; Turon and Londeix, 1988; Rochon, 1997; Abidi, Lezine, and Turon, unpubl. data). *B. tepikiense* is never abundant in modern sediments. Nevertheless, its presence seems to be related to cool winter environments (surficial water temperature often lesser than 10°C) and temperate summer environments (Edwards and Andrle, 1992; de Vernal et al., 1994). Its present-day optimal developments are recorded east of New Zealand (≈1%; Sun and McMinn, 1994) and south of Newfoundland (≈1%–12%; de Vernal and Turon, unpubl. data). In both cases, *B. tepikiense* is present in areas with oceanic convergences that induce meeting cold superficial waters (e.g., Labrador Stream, subantarctic water) and warmer waters (e.g., Gulf Stream, subtropical water). On the other hand, *S. mirabilis* s.l. and *Impagidinium patulum* can be considered as temperate to tropical taxa (Turon, 1984; Edwards and Andrle, 1992; Mudie and Harland, 1996).

During the Pleistocene, assemblages with abundant *N. labyrinthea* and *B. tepikiense* alternate with assemblages showing optimal relative abundances of *S. mirabilis* s.l. (Fig. 2). In the latter assemblages, *I. patulum* and *Selenopemphix nephroides* often show their optimal abundance. The W/C curve (see "Material and Methods" section) permits such dinocyst assemblage variations to be interpreted in terms of sea-surface temperature evolution. Thus, low-value in-

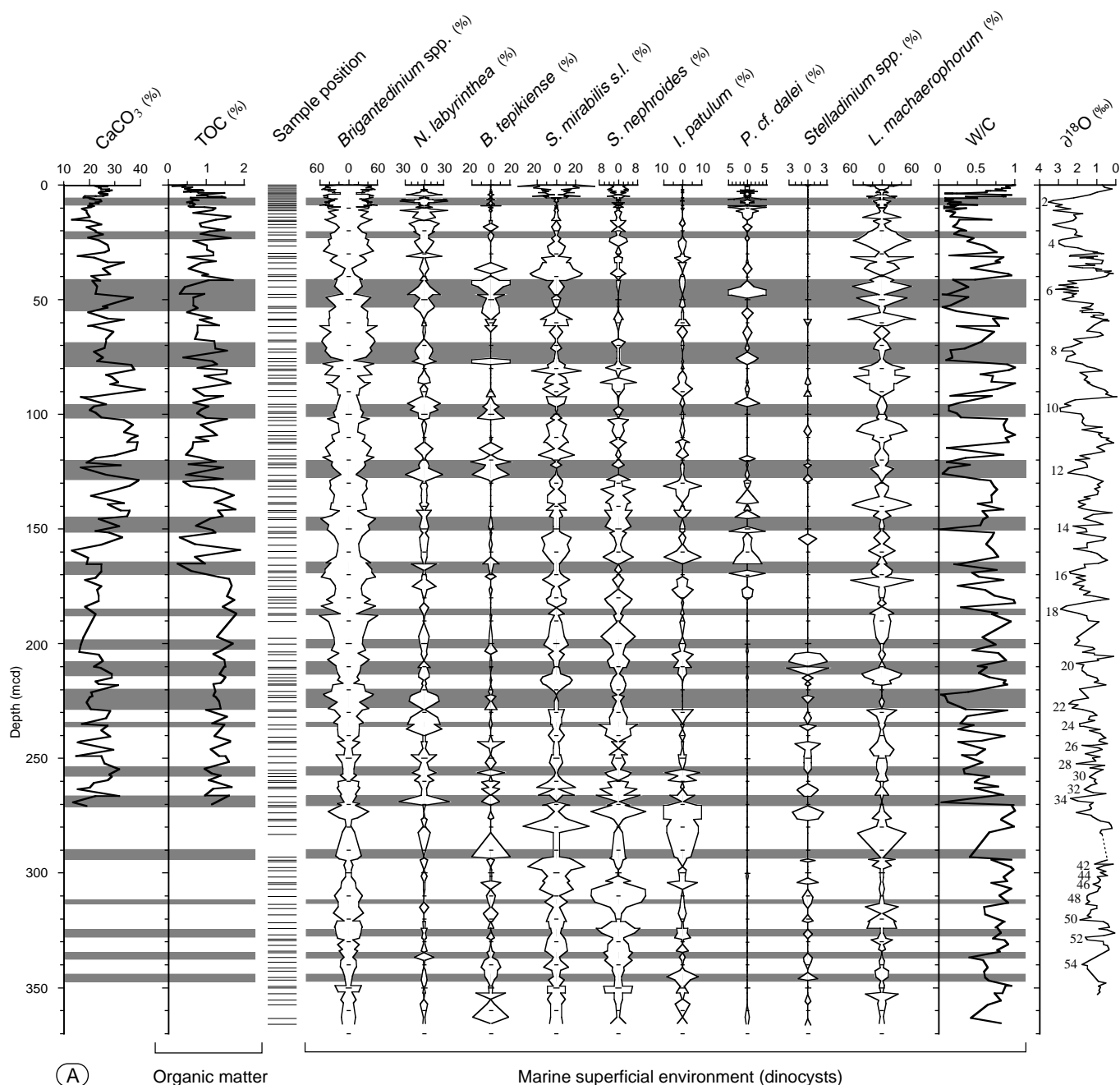


Figure 2. The Pleistocene and the Holocene record from Site 976. **A.** Depth plot of the sedimentary carbonate (%), total organic carbon (%), relative abundance (%) of selected dinocysts, warm vs. cool water indicating dinoflagellate cyst curves (W/C) taxa, and $\delta^{18}\text{O}$ record (*G. bulloides*) from Pleistocene sediments of Site 976. (Continued next page.)

tervals of the W/C value correspond to cooler periods (Fig. 2). Their frequency and stratigraphic location present the possibility that they might be the repercussion of Northern Hemisphere glaciations in the Mediterranean Sea. Cyclicity in the W/C value is well expressed in the upper 180 mcd of the Site 976 composite core: eight significant cool periods can be drawn (Fig. 2). On the basis of the W/C curve, such cycles appear to be badly expressed downward below 180 mcd; nevertheless, at least 12 cool periods can be considered significant indicators of cooler environments according to a concomitant increase in *N. labyrinthea* and *B. tepikiense* and decrease in *S. mirabilis* s.l. percentages. It is of note that a sharp change in dinocyst assemblages occurs around 180 mcd. In the lower part of the Pleistocene sequence, *Stelladinium* spp. are regularly present (even low percentages),

whereas above they are nearly absent. It is the opposite for *Pentaparsodinium* cf. *dalei* and *Algidasphaeridium*? cf. *minutum*, which are regularly recorded above 180 mcd and are nearly absent in underlying sediments. As recorded in modern sediments, *P. cf. dalei* and *A. ? minutum* are species adapted to low surface-water temperature (de Vernal et al., 1994; Mudie and Harland, 1996), whereas *Stelladinium* spp. shows its maximum abundance in the Persian Gulf and northeast and northwest borders of the Arabian Sea (Bradford and Wall, 1984; Zonneveld, 1996). Zonneveld (1996) counts *Stelladinium* spp. among northeast-monsoon eutrophic species. The relay observed around 180 mcd between these taxa may correspond to a climatic cycle with a longer term than those recorded with the W/C curve.

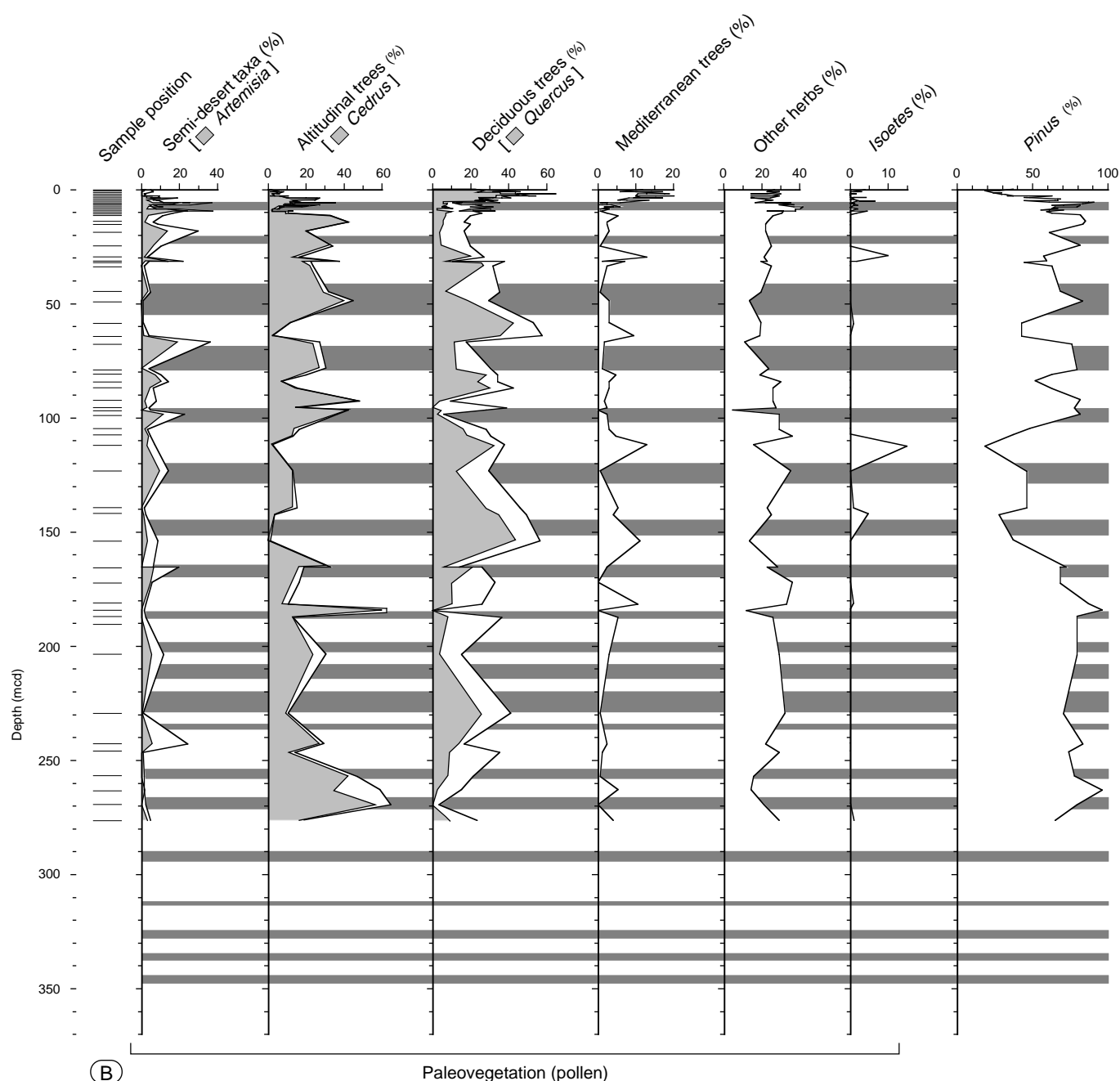


Figure 2 (continued). **B.** Relative abundance (%) of some pollen taxa from Pleistocene sediments of Site 976. Dinocyst percentages are calculated on a sum excluding *Lingulodinium machaerophorum*; *L. machaerophorum* percentages are calculated on the total dinocyst sum. Pollen percentages of *Pinus* are calculated on the total pollen sum and others on a sum excluding *Pinus*. Shaded areas correspond to periods of significant cooling as indicated by dinoflagellate cyst assemblages.

Relative abundance of *L. machaerophorum* cysts (number of *L. machaerophorum* specimens vs. total dinocyst sum) fluctuates all over the Site 976 Pleistocene sequence, from few percent to 76% (at 58.41 mcd; Fig. 2). Peaks of *L. machaerophorum* relative abundance seem to occur with an almost regular periodicity. The frequency of such peaks averages 27 m, which, according to the average sedimentation rate of the Pleistocene sequence (206 to 208 m/Ma; Comas, Zahn, Klaus, et al., 1996), corresponds to a ~130 ka mean periodicity. That is particularly well expressed between 220 and 60 mcd, and seems independent of climatic cyclicity as expressed by the W/C curve. The probably shallow-water origin of *L. machaerophorum* might allow one to interpret the peaks of this species as more or less

regular inputs of neritic water in the center of the Western Alboran Basin.

The detailed analyses of the uppermost 10 m of the Site 976 composite core allows one to distinguish several units on the basis of changes in palynological assemblages (Fig. 3). As in the underlying sediments, dinocyst assemblages of the upper 10 mcd are overwhelmingly dominated by *Brigantedinium* spp. Only relative abundance of other more significant species are only presented.

1. From 10 to 7.5 mcd, dinocyst assemblages are dominated (except *Brigantedinium* spp.) by *N. labyrinthea* and *B. tepikiense*. No significant variation occurs, except a peak of *B. tepikiense*

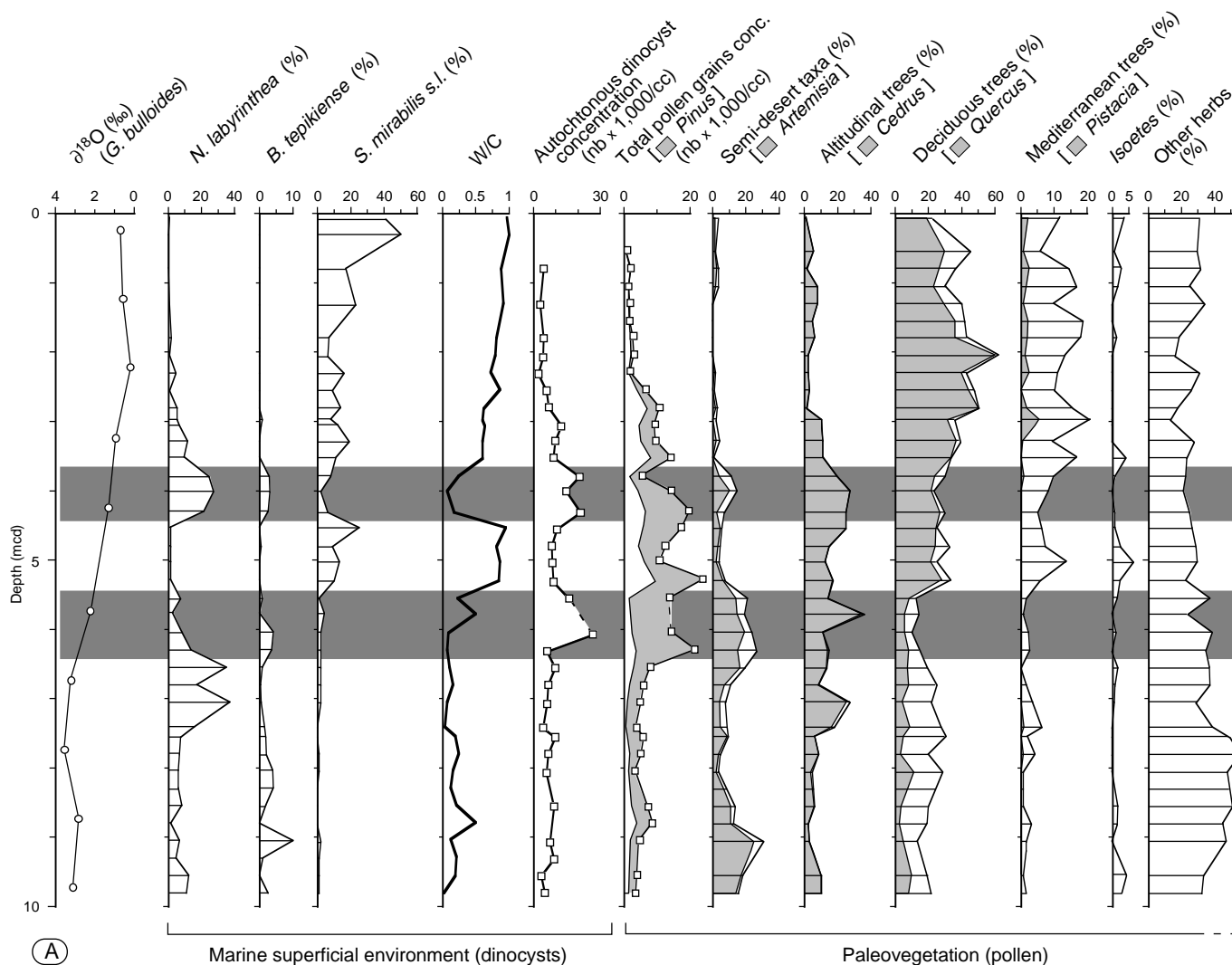


Figure 3. The last deglaciation. A. Changes in relative abundance (%) of selected dinocysts, warm vs. cool water indicating dinoflagellate cysts curve (W/C), autochthonous dinocyst then total pollen grains concentrations and relative abundance (%) of selected pollen types. (Continued next page.)

- at 9.05 mcd. The dinocyst concentrations are low, ranging from 3070 to 9130 cysts/cm³.
- 2. From 7.41 to 6.55 mcd, *N. labyrinthea* percentages increase sharply (up to 38%). No sharp variation is shown by other dinocyst percentages during this interval.
- 3. From 6.30 to 5.55 mcd, *N. labyrinthea* percentages decrease, whereas *B. tepikiense* become more abundant. Concurrently, dinocyst concentrations reach highest values, up to 26,250 cysts/cm³. Dinocyst concentrations are considered as indicators of variability in sea-surface water nutrient abundance and then in primary productivity. Such height values in this interval probably indicate enhanced primary productivity.
- 4. From 5.29 to 4.3 mcd, percentages of the warm species *S. mirabilis* s.l. increase significantly (up to 25%), which indicates a slight warming of the sea-surface waters. The concentrations of dinocysts are again low.
- 5. From 4.3 to 3.79 mcd, a concomitant increase of *N. labyrinthea* and *B. tepikiense* percentages and of dinocyst concentrations (averaging 18,480 cyst/cm³) marks cooler sea-surface water with enhanced primary productivity.

- 6. Above 3.79 mcd, dinocyst concentrations and *N. labyrinthea* percentages decrease progressively, whereas that of *S. mirabilis* s.l. increase. The present-day hydrological and climatic conditions progressively settle in the western Alboran Sea.

Paleovegetation

Because of the central location of Site 976 within the Alboran Sea, the pollen-source area is believed to be mainly northern Moroccan and southern Spanish borderlands. Ninety-seven pollen taxa have been determined, and the pollen spectra range from a semidesert assemblage to those of deciduous and coniferous forests (Figs. 2, 3). The pollen diagram reflects the competition of four main vegetation groups, which were distributed in an altitudinal organization similar to that of today. Among the herbaceous group, which does not constitute a homogeneous unit, high percentages of *Artemisia*, *Ephedra*, and *Chenopodiaceae* may reflect the expression of a steppe or a semi-desert extension (e.g., Walter, 1974; Bottema, 1974). The Mediterranean forest is documented by pollen of *Olea*, *Phillyrea*, *Cistus*, *Quercus ilex*, and *Pistacia*. In an altitudinal scheme, they are located at

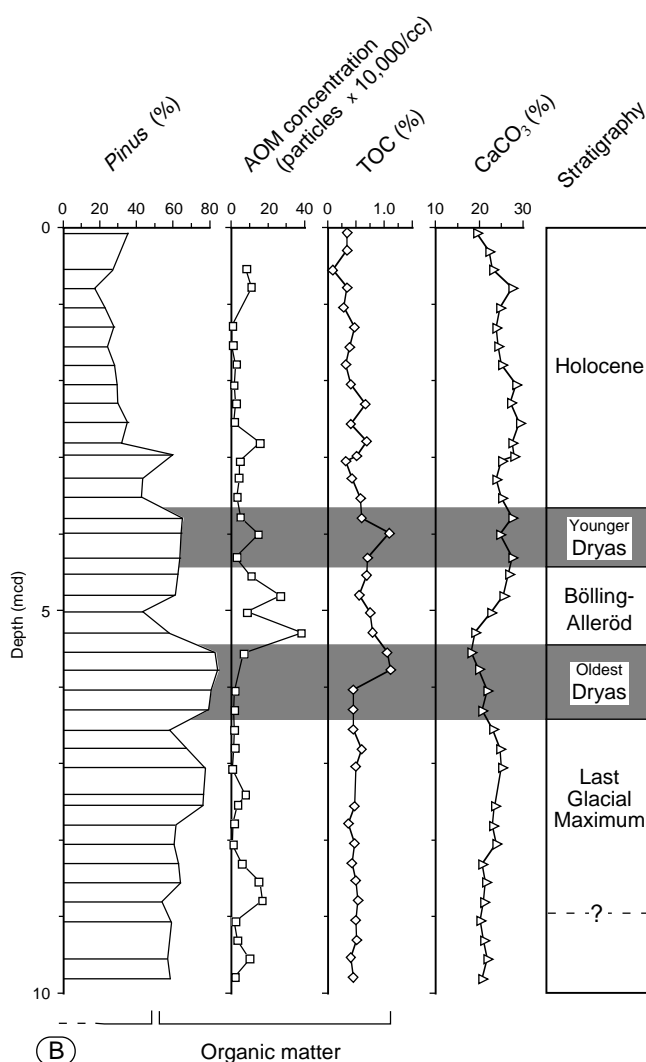


Figure 3 (continued). **B.** Relative abundance (%) of *Pinus* pollen grains, amorphous organic matter concentration, total organic carbon (%), sedimentary carbonate (%), $\delta^{18}\text{O}$ record (*G. bulloides*), and deduced stratigraphy in the upper 10 mcd from Site 976. Dinocyst percentages are calculated on a sum excluding *Lingulodinium machaerophorum*. Pollen percentages of *Pinus* are calculated on the total pollen sum and others on a sum excluding *Pinus*.

lower altitudes back to the coastal formation. The *Quercus* (oak) forest, which was extended at the mid-altitudes, is mainly represented by deciduous *Quercus* species associated with Ericaceae. Pollen of other trees are more often rare. The coniferous forest is represented mainly by *Cedrus*, sometimes accompanied by *Abies* in the lowermost samples and rarely by *Picea*; this forest occupied the highest elevations of the Rif and Betic Cordillera, as it does today. *Pinus* was probably mixed as well in the *Quercus* forest as it was in the coniferous forest.

During the Pleistocene (Fig. 2), high percentages of pollen of semidesert taxa alternate with those of forest species, especially those of the mid-altitude *Quercus* forest. These replacements express the repeated extension and retreat of mid-altitude forest in opposition to the semidesert assemblages on the Alboran Sea borderlands. At least eight clear oscillations are depicted in the pollen diagram of the upper 180 mcd sediments. Below this depth, the vegetation signal is difficult to interpret because of the wide interval between samples. Below

180 mcd, the composition of the coniferous forest appears modified with more abundant *Abies* concurrent with high *Pinus* percentages (averaging 80%). In the upper samples, *Pinus* percentages regularly oscillate between 40% and 90%.

Detailed analyses of the uppermost 10 m show several paleovegetational phases (Fig. 3).

1. From 10 to 9.10 mcd, pollen of grasses (especially Asteraceae) and deciduous trees are equally represented. Coniferous forest is represented by *Cedrus*, which reaches 10%. *Isoetes* is present. The Alboran Sea coasts are occupied by a grass open vegetation replaced in mid-altitudes by the forest on the Rif and the Betic Cordillera slopes.
2. From 9.05 to 8.8 mcd, *Artemisia* reaches its highest percentage (about 27% at 9.05 mcd) and Chenopodiaceae representation increases. Tree pollen, except *Pinus* grains, are in very low percentages. In Morocco and southern Spain lands are occupied by a semidesert widely extended at all altitudes, and the forest is restricted to sheltered areas.
3. From 8.8 to 6.55 mcd, steppe elements are in low percentages while Cichorioideae reach high percentages (more than 30%) and dominate the open vegetation association. Ericaceae percentages reach their highest values (20%). High percentages of *Cedrus* are recorded at 5.77 mcd. *Isoetes* is present. The mid-altitude forest is slightly extended, while an open vegetation is widely developed around the Alboran Sea.
4. From 6.55 to 5.55 mcd, *Artemisia* percentages increase again and are accompanied by *Ephedra* and Chenopodiaceae in high abundances. Cichorioideae and Poaceae, decrease strongly. Ericaceae and *Quercus* are in low abundance, whereas *Pinus* is still highly represented. The semidesert is largely extended in the Moroccan and southern Spain edges. The deciduous forest is restricted to sheltered areas.
5. From 5.55 to 4.3 mcd, *Pinus* and coniferous trees decrease. Deciduous *Quercus* representation increase in the first step and is accompanied by the Mediterranean trees, especially *Quercus ilex*. Herbs are low represented and *Artemisia* decrease strongly. *Pinus* percentages decrease. *Isoetes* reaches its highest values (7%). The mid-altitude *Quercus* forest begins to extend in the Rif mountains and Betic Cordillera. The semidesert is then restricted to the coast. During this period, pollen concentrations reach their highest values.
6. From 4.35 to 3.5 mcd., *Artemisia*, *Ephedra*, and Chenopodiaceae increase again. *Quercus*, which remains the dominant taxa of the deciduous forest, slightly decrease in percentages. *Cedrus* is better represented. The semidesert extends again. The *Quercus* forest, although less developed, still occupies the mid-altitudes while the coniferous forest is more extended.
7. After 3.5 mcd the mid-altitude forest, and especially *Quercus*, increases again in percentages. *Pinus* is abundant up to 2.8 mcd and then decreases. In the same period, *Artemisia* and Chenopodiaceae persist in low percentages while the other herbaceous elements remain in almost the same percentages. At 2.8 mcd, the first peak of *Pistacia* percentages is recorded. This event is correlated to a peak in total pollen concentrations. Mediterranean plants such as *Olea*, *Phillyrea*, and *Cistus* accompany *Quercus ilex*, which here reaches its highest representation. Between 2.55 and 2.05 mcd, deciduous *Quercus* has its highest percentages. Above 2.05 mcd, *Quercus* slightly decreases and is replaced by Ericaceae.

This vegetation succession expresses the progressive setting of the Holocene vegetation in the borderlands of the Alboran Sea. The semidesert is progressively reduced to a coastal belt while the conif-

erous forest, probably dominated at this time by *Pinus*, is rapidly replaced by the deciduous *Quercus* and the Mediterranean forests. This pollen succession is fairly comparable to those recorded in southern Spain and northern Morocco (Pons and Reille, 1988; Lamb et al., 1989; Reille, 1990).

Organic Matter

Carbonate Carbon

Concentrations of carbonate carbon vary between 1.6% and 5.0%, with a mean value around 3.0%. Such concentrations are equivalent to 13% to 42% sedimentary CaCO_3 , assuming that all of the carbonate is present as pure calcite or aragonite.

The curve of the calcium carbonate content (Fig. 2) shows high amplitude variations, ranging from 18% to 27%, between 270 and 160 mcd. The mean content of calcium carbonate increases between 160 and 75 mcd, with higher amplitude variations, ranging from 21% to 36%. From 75 to 15 mcd, the variations in carbonate content are lower and show a general decreasing trend that reaches a minimum value of 13% at 15.13 mcd. In the uppermost 10 m (Fig. 3), the carbonate content slightly increases up to 25% at 7 mcd, then decreases down to 18% at 5.55 mcd. Between 5.55 and 4.80 mcd, the carbonate content increases and then shows slight variations up to 2.55 mcd. From this depth to the top, the calcium carbonate content is decreasing from 28.7% to 19.3%.

Organic Carbon

Concentrations of organic carbon vary between 0.1% and 1.9%, with a mean value around 1.0% TOC. Similar range in organic carbon content was recorded on board the *JOIDES Resolution* (Comas, Zahn, Klaus, et al., 1996), although our mean value is slightly higher. The TOC record reflects the quantity of organic matter, although it should be kept in mind that organically bound oxygen, hydrogen, sulfur, and nitrogen can contribute up to 50% of the total sedimentary organic matter.

During the Pleistocene, the organic carbon content (Fig. 2) shows that TOC values are high (1.25% average) between 270 and 170 mcd and exhibits a general increase from the bottom to the top of this interval. At this depth, the TOC content decreases sharply (down to 0.6%). From 170 to 10 mcd, the TOC content shows high-amplitude fluctuations. Five peaks of organic carbon enrichment are recorded near 140, 100, 80, 40, and 15 mcd. These peaks are not necessarily correlated with those of the calcium carbonate.

In the uppermost 10 m, the organic carbon content shows two peaks centered on 5.29 and 4.00 mcd. From this depth to the top, the TOC content is decreasing from 1.5% to 0.45%. A slight peak reaching 0.92% is recorded at 2.8 mcd.

These ranges in carbonate and organic carbon contents reflect a combination of fluctuating biological productivity, dilution by non-carbonate sedimentary supply, and post-depositional effects, such as carbonate dissolution and organic matter oxidation.

Hydrogen index (HI) and source of the organic matter

Hydrogen index is considered to be the most reliable Rock-Eval pyrolysis parameter for typing the sedimentary organic matter (Espitalié et al., 1986). However, it should be noted that for siliciclastic whole-rock samples, HI is often too low where TOC contents are below 0.5% as a result of the so-called "matrix effect," which is a retention of hydrocarbons by clay minerals (Peters, 1986). In order to correct for "matrix effect," Langford and Blanc-Valleron (1990) suggest that the mean HI should be determined from the regression of S2 and TOC data. This line is presented for the last 10 mcd on Fig. 4, which clearly indicates that the sediments contain type III (land-derived) or type IV (deeply altered) organic matter (Tissot and Welte, 1984).

Both low TOC and HI values suggest that the studied samples contain a mixture of terrestrial and deeply oxidized marine organic matter. This interpretation is fully supported by the palynological observations that reveal more than 50% of the organic particles are terrestrial in origin.

Amorphous Organic Matter

In the upper 10 mcd, the amorphous organic matter (AOM) concentrations oscillate from values lower than 1,000 particles per gram to 30,000 particles per gram of sediments. Higher values are reached between 9.7 and 8 mcd, at 5.29 mcd, between 5 mcd to 3.8 mcd, and at 2.8 mcd and 0.79 mcd. Two of these peaks are correlated to high TOC and HI at 4, and 2.8 mcd. Nevertheless, the first organic carbon enrichment, recorded at 5.29 mcd, coincides with the lowest HI values and low calcium carbonate content, whereas the second (around 4.00 mcd) corresponds to the highest HI values of the uppermost 10 m. At the state of our study it is not clear if this relationship is controlled by dilution effect or if different types of AOM exist in the palynofacies.

CLIMATIC AND HYDROLOGICAL INTERPRETATION

The Last Deglaciation (0–10 mcd)

According to the chronology proposed in the initial biostratigraphic framework (Comas, Zahn, Klaus, et al., 1996) and to the age model developed by von Grafenstein and Zahn and others (herein and Chap. 37, this volume), our detailed record of the uppermost 10 mcd can be related to the last 28 cal ka. Thus, the modifications in dinocyst assemblages and in vegetation express the successive climatic changes that have occurred from the Last Glacial Maximum to the present day.

1. The 10 to 6.55 mcd interval is related to the Last Glacial Maximum. The climate was cool as evidenced by the wide extension of the open herbaceous vegetation with Cichorioideae and the presence of Ericaceae. Moisture was available, especially in high elevations, as demonstrated by the presence of altitudinal trees such as *Cedrus* in the uppermost samples of this interval. Concurrently, the few percent of *Isoetes* indicate inputs of fresh water. At 9.05 mcd, a peak of *Artemisia* expressed a short-term aridity event. At the same time, *B. tepikiense* abundance reveals a strong thermic

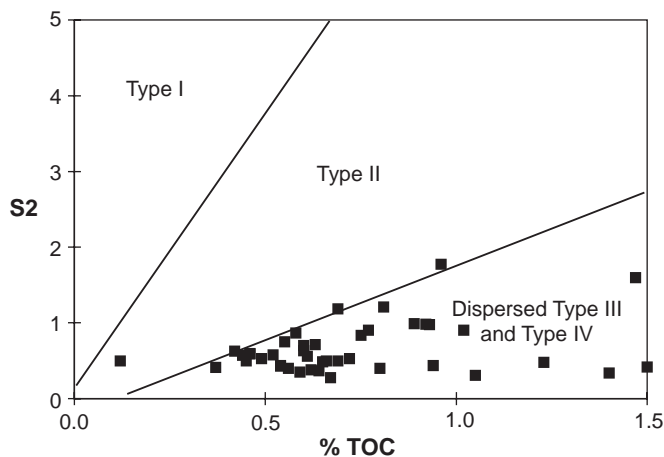


Figure 4. Kerogen type of samples from the uppermost 10 mcd at Site 976 as defined by the cross-plot of TOC and pyrolysis S2 parameter (after Langford and Blanc-Valleron, 1990).

- gradient in the sea-surface waters. From 7.55 to 6.55 mcd, sea-surface temperature is cooler than previously as shown by the W/C curve. That interval might correspond to the Last Glacial Maximum.
2. From 6.35 mcd to 5.55 mcd, climate changes toward cool conditions on the continents as well as in the sea-surface waters. Aridity is maximum with the highest extension of the semidesert on land. The cooling of the sea-surface is marked by the reoccurrence of *B. tepikiense*. This event unequivocally corresponds to the Oldest Dryas, already recognized in the peat bog records of Padul (Pons and Reille, 1988) and in other Mediterranean records (e.g., de Beaulieu and Reille, 1983; Reille, 1990; Wijmstra, 1969; Willis, 1994; Watts et al., 1996). In our record, it can be dated between ~18.5 cal ka and ~6.4 cal ka. At similar depth, a correlative modification in the foraminiferal assemblages indicates a cooling of the sea-surface temperatures (Capotondi and Vigliotti, Chap. 40, this volume). The beginning of this period coincides with the large discharge of icebergs in the North Atlantic, Heinrich event H1 (Bond et al., 1993; Grousset et al., 1993).
 3. From 5.55 to 4.35 mcd (~16.4 cal ka to ~12.7 cal ka), a clear climatic improvement is marked by the extension of the deciduous forest and the Mediterranean forest on the Alboran Sea borderlands. In marine environments, it is expressed by the abundance of *S. mirabilis*. As in the Padul peat bog (Pons and Reille, 1988), this improvement is more pronounced in the western Mediterranean Sea than in other Mediterranean sites. The increase in humidity is shown by high percentages of *Isoetes*, which expresses freshwater supply from the continent. This interval is related to the Bölling/Alleröd late glacial interstadial.
 4. From 4.35 to 3.6 mcd (~12.7 cal ka to ~10.6 cal ka), the re-extension of the *Artemisia*-rich semidesert, in Spain and Morocco landscapes, express the return of aridity. In the same interval, the Alboran Sea surface temperature decreases as shown by the concomitant development of *N. labyrinthea* and *B. tepikiense*. This interval corresponds to the Younger Dryas event. A correlative modification in the foraminiferal assemblages indicates a cooling of the sea-surface temperatures (Capotondi and Vigliotti, Chap. 40, this volume). In other Mediterranean sites (Turon and Londeix, 1988; Pujol and Vergnaud Grazzini, 1989; Vergnaud Grazzini and Pierre, 1991; Combourieu Nebout et al., 1998), the Younger Dryas is better expressed by the palynological record than by the $\delta^{18}\text{O}$ record, probably because of the higher resolution sampling of the combined pollen and dinocyst record. In Site 976, the lower resolution sampling for $\delta^{18}\text{O}$ values does not allow the Younger Dryas to be detected.
 5. Above 3.6 mcd, the onset of Holocene is marked by the progressive extension of the deciduous forest elements and the retreat of both coniferous forest and semidesert. The highest representation of *Quercus* between 2.55 and 2.05 mcd marks the climatic optimum.
 6. At 2.8 mcd, a peak of *Pistacia*, a Mediterranean tree linked to mild winter climatic conditions (UNESCO, 1968) indicates the increase of winter temperatures. This first occurrence, widely observed in the Mediterranean area, is dated here at about 8.9 cal ka which appears younger than in other Mediterranean sites (Bottema, 1974; Willis, 1994; Reille and Lowe, 1993; Rossignol-Strick et al., 1992; Rossignol-Strick, 1995). At 2.8 and 4.0 mcd correlative high concentrations in amorphous organic matter, high values in both TOC and HI, high total pollen concentrations may represent the virtual expression of two organic-rich layers, although color change and magnetic susceptibility anomalies are observed only between 3.60 and 4.5 mcd (Murat, Chap. 41, this volume).

During the last deglaciation, aridity increased on the Moroccan and Spain lands, and sea-surface temperature decreased in the Alboran Sea at 9.05 mcd, between 6.55 and 5.55 mcd, and between 4.3 and

3.6 mcd. The two last events are correlated to peaks in dinocyst concentrations, which indicate enhanced primary productivity in the sea-surface waters. They are also correlated to peaks in TOC, which may express an increase of organic matter flux. As demonstrated by Turon and Londeix (1988), such arid and cool events involved increasing evaporation of sea-surface waters, then to an increase of sea-surface salinity, and a decrease of surficial temperature (which presently occurs during coolest winter with evaporation enhanced by mistral and tramontane winds). These environmental conditions led to an intensification of vertical convection, particularly in the areas of bottom-water formation (i.e., Ligurian Sea), and then induced an increased renewal of bottom waters and an enhanced inflow of surficial Atlantic waters in the Alboran Sea. This intensification of Atlantic/Mediterranean exchanges led to an enrichment in the sea-surface water nutrients of the Alboran Sea, triggering enhanced primary productivity. Although arid, the oldest event (at 9.05 mcd) is not correlated to peaks in dinocyst concentrations, nor to an increasing TOC value, and cannot be interpreted as reflecting high productivities in the Alboran Sea.

The Pleistocene

The cyclic alternations observed in the dinocyst and pollen assemblages is, without any doubt, related to the Pleistocene glacial/interglacial cyclicity, as expressed by the fair correlation between W/C value and $\delta^{18}\text{O}$ curve. That cyclicity is well marked from top to 240 mcd with highest amplitudes between 0 and 180 mcd. Below 240 mcd the climatic signal is less readable. The change in the dinocyst flora at 180 mcd of the near-disappearance of *Stelladinium* spp., along with the appearance of *P. cf. dalei*, reflects a major event that is dated at about 700 cal ka according to the age model of von Grafenstein et al. (Chap. 37, this volume). It is noteworthy that *Stelladinium* spp. cysts from modern sediments of Arabian Sea are associated with eutrophic conditions during northeast monsoons (Zonneveld, 1996). In addition, constant high values of TOC occur at almost the same depth. That may be interpreted as an organic matter enrichment caused by the compaction of sediments, as better preservation, or as an increase in productivity. The magnetic susceptibility and density (measured with the gamma-ray attenuation porosity evaluator [GRAPE]; Comas, Zahn, Klaus, et al., 1996) do not show a strong change during that period, which implies that the changes recorded in the TOC does not relate to a diagenetic problem. It is of note that the cysts of *Brigantedinium* spp. are among the less resistant ones (Turon, 1984; Marret, 1993). They are highly represented from top to 180 mcd (up to 71%), but then their percentages decrease below that limit. Such decrease in *Brigantedinium* cysts percentages do not support the hypothesis of better preservation of the organic material during the 180–366 mcd interval. So, according to dinocyst and organic matter records, it seems the sea-surface floral change occurring at 180 mcd may correspond to a sharp hydrological and/or climatic change, which may have led to a modification of the marine productivity.

CONCLUSIONS

The palynological record of Site 976 documents the continental and marine paleoenvironmental changes that occurred in the Alboran Sea Basin during the Pleistocene and the Holocene. Vegetation changes on the Alboran Sea borderlands and modifications in the dinocyst flora record several glacial/interglacial cycles during the upper Pleistocene. An abrupt change in the marine flora occurs at about 700 cal ka, which may be related to a sharp hydrological change in the sea-surface waters. The high-resolution record of the last 28 cal ka exhibits the classic climatic steps from the Last Glacial Maximum to the Holocene. Three aridity phases shown by the extension of the semidesert vegetation on the Alboran Sea borderlands are correlated

to cooling of the sea-surface waters marked by the development of the dinocysts *Nematosphaeropsis labyrinthea* and/or *Bitectatodinium tepikiense*. The two upper phases correspond to the Oldest Dryas and Younger Dryas and are marked by increased primary productivity, which are depicted by the higher concentrations in dinocysts and high values of TOC.

ACKNOWLEDGMENTS

The authors received financial support from the Centre National de la Recherche Scientifique and from the universities of Bordeaux I and Paris VI. That research was supported by the Geosciences Marines program of the Institut National des Sciences de l'Univers. We thank the Ocean Drilling Program for making the samples available for that project and the shipboard party of Leg 161 for assistance in sampling. We thank A. de Vernal and J. Matthiessen for their critical reviews of this paper. We gratefully acknowledge J. Sanfourche, M.H. Castera, and J.P. Cazet for their efficient technical assistance.

REFERENCES

- Andrieuff, P., Bouysse, P., Châteauneuf, J.J., L'Homer, A., and Scolari, G., 1971. La couverture sédimentaire meuble du plateau continental externe de la Bretagne méridionale (Nord du Golfe de Gascogne). *Cah. Oceanogr.*, 23:343–381.
- Barbero, M., Quezel, P., and Rivaz Martinez, S., 1981. Contribution à l'étude des groupements forestiers et préforestiers de Maroc. *Phytoenologia*, 9:311–412.
- Benabib, A., 1982. Bref aperçu sur la zonation altitudinale de la végétation climatique du Maroc. *Ecol. Mediterr.*, 8:301–315.
- Béthoux, J.P., 1979. Budgets of the Mediterranean Sea: their dependence on the local climate and the characteristics of the Atlantic waters. *Oceanol. Acta*, 2:157–163.
- Béthoux, J.-P., and Prieur, L., 1984. Hydrologie et circulation en Méditerranée nord-occidentale. In Bizon, J.J., and Burolet, P.F., et al. (Eds.), *Ecologie des Microorganismes en Méditerranée Occidentale*: ECOMED, Assoc. Franc. Tech. Petrole, 13–22.
- Biebow, N., 1996. Dinoflagellatenzyklen als Indikatoren der Spät- und Postglazialen Entwicklung des Auftretensgeschehens vor Peru. *Geomar Rep.*, 57:1–100.
- Bond, G., Broecker, W., Johnsen, S., McManus, J., Labeyrie, L., Jouzel, J., and Bonani, G., 1993. Correlations between climate records from the North Atlantic sediments and Greenland ice. *Nature*, 365:143–147.
- Bottema, S., 1974. Late Quaternary vegetation History of North-western Greece [Thesis Doctorate]. Univ. Groningen.
- Bradford, M.R., and Wall, D.A., 1984. The distribution of Recent organic-walled dinoflagellate cysts in the Persian Gulf, Gulf of Oman, and north-western Arabian Sea. *Palaeontographica B*, 192:1–84.
- Brooks, J., 1971. Some chemical and geochemical studies on sporopollenin. In Brooks, J., Grant, P.R., Muir, M.D., Van Gijzel, P., and Shaw, G. (Eds.), *Sporopollenin*: London (Academic Press), 351–407.
- Comas, M.C., Zahn, R., Klaus, A., et al., 1996. *Proc. ODP, Init. Repts.*, 161: College Station, TX (Ocean Drilling Program).
- Combourieu Nebout, N., Paterne, M., Turon, J.L., and Siani, G., 1998. A high resolution record of the Last Deglaciation in the Central Mediterranean Sea: palaeovegetation and palaeohydrological evolution. *Quat. Sci. Rev.*, 17:303–317.
- de Beaulieu, J.L., and Reille, M., 1983. Paléoenvironnement tardiglaciaire et Holocène des lacs de Pélautier et Siguret (Hautes-Alpes, France): histoire de la végétation d'après les analyses polliniques. *Ecol. Mediterr.*, 9:16–36.
- de Vernal, A., Turon, J.-L., and Guiot, J., 1994. Dinoflagellate cyst distribution in high-latitude marine environments and quantitative reconstruction of sea-surface salinity, temperature, and seasonality. *Can. J. Earth Sci.*, 31:48–62.
- Duplessy, J.C., Delibrias, G., Turon, J.L., Pujol, C., and Duprat, J., 1981. Deglacial warming of the North-eastern Atlantic Ocean: correlation with the paleoclimatic evolution of the European continent. *Palaeogeogr., Palaeoclimatol., Palaeoecol.*, 35:121–144.
- Edwards, L.E., and Andrieu, V.A.S., 1992. Distribution of selected dinoflagellate cysts in modern marine sediments. In Head, M.J., and Wrenn, J.H. (Eds.), *Neogene and Quaternary Dinoflagellate Cysts and Acritarchs*. Am. Assoc. Stratigr. Palynol. Found., 259–288.
- Espitalié, J., Deroo, G., and Marquis, F., 1985a. La pyrolyse Rock-Eval et ses applications, Partie I. *Rev. Inst. Fr. Pet.*, 40/5:563–579.
- , 1985b. La pyrolyse Rock-Eval et ses applications, Partie II. *Rev. Inst. Fr. Pet.*, 40:755–784.
- , 1986. La pyrolyse Rock-Eval et ses applications, Partie III. *Rev. Inst. Fr. Pet.*, 41:73–89.
- Grousset, F.E., Labeyrie, L., Sinko, J.A., Cremer, M., Bond, G., Duprat, J., Cortijo, E., and Huon, S., 1993. Patterns of ice-rafted detritus in the glacial North Atlantic (40°–55°N). *Paleoceanography*, 8:175–192.
- Harland, R., 1983. Distribution maps of recent dinoflagellate cysts in bottom sediments from the North Atlantic Ocean and adjacent seas. *Palaeontology*, 26:321–387.
- Hodell, D.A., and Venz, K., 1992. Toward a high-resolution stable isotopic record of the Southern Ocean during the Pliocene-Pleistocene (4.8 to 0.8 Ma). In Kennett, J.P., Warnke, D.A. (Eds.), *The Antarctic Paleoenvironment: A Perspective on Global Change* (Pt. 1). Am. Geophys. Union, Antarct. Res. Ser., 56:265–310.
- Imbrie, J., Hays, J.D., Martinson, D.G., McIntyre, A., Mix, A.C., Morley, J.J., Pisias, N.G., Prell, W.L., and Shackleton, N.J., 1984. The orbital theory of Pleistocene climate: support from a revised chronology of the marine $\delta^{18}\text{O}$ record. In Berger, A., Imbrie, J., Hays, J., Kukla, G., and Saltzman, B. (Eds.), *Milankovitch and Climate* (Pt. 1), NATO ASI Ser. C, Math Phys. Sci., 126: Dordrecht (D. Reidel), 269–305.
- Kobayashi, S., Matsuoka, K., and Iizuka, S., 1986. Distribution of dinoflagellate cysts in surface sediments of Japanese coastal waters. I. Omura Bay, Kyushu. *Bull. Plankton Soc. Jpn.*, 33:81–93.
- Lacombe, H., and Tchernia, P., 1972. Caractères hydrologiques et circulation des eaux en Méditerranée. In Stanley, D.J. (Ed.), *The Mediterranean Sea: a Natural Sedimentation Laboratory*: Stroudsburg, PA (Dowden, Hutchinson and Ross), 25–36.
- Lamb, H.F., Eicher, U., and Switsur, V.R., 1989. An 18,000-year record of vegetation, lake-level and climatic change from Tigmilme, Middle Atlas, Morocco. *J. Biogeogr.*, 16:65–74.
- Langford, F.F., and Blanc-Valleron, M.M., 1990. Interpreting Rock-Eval pyrolysis data using graphs of pyrolyzable hydrocarbons vs. total organic carbon. *AAPG Bull.*, 74:799–804.
- Lewis, J., Dodge, J.D., and Powell, A.J., 1990. Quaternary dinoflagellate cysts from the upwelling system offshore Peru, Hole 686B, ODP Leg 112. In Suess, E., von Huene, R., et al., *Proc. ODP, Sci. Results*, 112: College Station, TX (Ocean Drilling Program), 323–328.
- Marret, F., 1993. Les effets de l'acétolyse sur les assemblages de kystes de dinoflagellés. *Palynosciences*, 2:267.
- Matsuoka, K., 1985. Organic-walled dinoflagellate cysts from surface sediments of Nagasaki Bay and Senzaki Bay, West Japan. *Bull. Fac. Lib. Arts, Nagasaki Univ., Nat. Sci.*, 25:21–115.
- Morzadec-Kerfourn, M.T., 1977. Les kystes de dinoflagellés dans les sédiments récents le long des côtes bretonnes. *Rev. Micropaleontol.*, 20:157–166.
- Mudie, P.J., 1992. Circum-Arctic Quaternary and Neogene marine palynofloras: paleoecology and statistical analysis. In Head, M.J., and Wrenn, J.H. (Eds.), *Neogene and Quaternary Dinoflagellate Cysts and Acritarchs*. Am. Assoc. Stratigr. Palynol. Foundation, 347–390.
- Mudie, P.J., and Harland, R., 1996. Aquatic Quaternary. In Jansonius, J., and McGregor, D.C. (Eds.), *Palynology: Principles and Applications*. Am. Assoc. Stratigr. Palynol. Foundation, 2:843–877.
- Ozenda, P., 1975. Sur les étages de végétation dans les montagnes du bassin méditerranéen. *Doc. Cartogr. Ecol.*, 16:1–32.
- Peters, K.E., 1986. Guidelines for evaluating petroleum source rock using programmed pyrolysis. *AAPG Bull.*, 70:318–329.
- Pons, A., and Reille, M., 1988. The Holocene and upper Pleistocene pollen record from Padul (Granada, Spain): a new study. *Palaeogeogr., Palaeoclimatol., Palaeoecol.*, 66:24–263.
- Pujol, C., and Vergnaud-Grazzini, C., 1989. Palaeoceanography of the Last Deglaciation in the Alboran Sea (Western Mediterranean): stable isotope and planktonic foraminiferal records. *Mar. Micropaleontol.*, 15:153–179.

- Reid, P.C., 1977. Peridiniacean and Glenodiniacean dinoflagellate cysts from the British Isles. *Nova Hedwigia*, 29:429–463.
- Reille, M., 1990. *Leçon de Palynologie et d'Analyse Palynologique*: (Paris) Ed. CNRS.
- Reille, M., and Lowe, J.J., 1993. A re-evaluation of the vegetation history of the Eastern Pyrenees (France) from the end of the glacial to the present. *Quat. Sci. Rev.*, 12:47–77.
- Rivas Martinez, S., 1982. La zonation altitudinale de la végétation de la péninsule ibérique, importance relative des facteurs bioclimatiques et chorologiques. *Ecol. Mediterr.*, 8:275–288.
- Rochon, A., 1997. Palynologie marine dans le Nord-Est de l'Atlantique Nord: distribution des kystes de dinoflagellés dans les sédiments récents et changements environnementaux le long des marges Sud Scandinaves au cours du dernier cycle climatique [Thèse Sci. Environ.]. Univ. Québec Montréal.
- Rossignol-Strick, M., 1995. Sea-land correlation of pollen records in the eastern Mediterranean for the glacial-interglacial transition: biostratigraphy versus radiometric time-scale. *Quat. Sci. Rev.*, 14:893–915.
- Rossignol-Strick, M., and Planchais, N., 1989. Climate patterns revealed by pollen and oxygen isotope records of a Tyrrhenian sea core. *Nature*, 342:413–416.
- Rossignol-Strick, M., Planchais, N., Paterne, M., and Duzer, D., 1992. Vegetation dynamics and climate during the Deglaciation in the South Adriatic Basin from a marine record. *Quat. Sci. Rev.*, 11:415–423.
- Ruddiman, W.F., Raymo, M.E., Martinson, D.G., Clement, B.M., and Backman, J., 1989. Pleistocene evolution: Northern Hemisphere ice sheets and North Atlantic ocean. *Paleoceanography*, 4:353–412.
- Ryan, W.B.F., Hsü, K.J., et al., 1973. *Init. Repts. DSDP*, 13 (Pts. 1 and 2): Washington (U.S. Govt. Printing Office).
- Sarnthein, M., Jansen, E., Weinelt, M., Arnold, M., Duplessy, J.C., Erlenkeuser, H., Flatøy, A., Johannessen, G., Johannessen, T., Jung, S., Koç, N., Labeyrie, L., Maslin, M., Pflaumann, U., and Schulz, H., 1995. Variations in Atlantic surface ocean paleoceanography, 50°–80°N: a time-slice record of the last 30,000 years. *Paleoceanography*, 10:1063–1094.
- Shaw, G., 1971. The chemistry of sporopollenin. In Brooks, J., Grant, P.R., Muir, M.D., Van Gijzel, P., and Shaw, G. (Eds.), *Sporopollenin*: London (Academic Press), 305–348.
- Sun, X., and McMinn, A., 1994. Recent dinoflagellate cyst distribution associated with the Subtropical Convergence on the Chatham Rise, east of New Zealand. *Mar. Micropaleontol.*, 23:345–356.
- Tiedemann, R., Sarnthein, M., and Shackleton, N.J., 1994. Astronomic timescale for the Pliocene Atlantic $\delta^{18}\text{O}$ and dust flux records of Ocean Drilling Program Site 659. *Paleoceanography*, 9:619–638.
- Tissot, B.P., and Welte, D.H., 1984. *Petroleum Formation and Occurrence* (2nd ed.): Heidelberg (Springer-Verlag).
- Turon, J.L., 1984. Le phytoplancton dans l'environnement actuel de l'Atlantique nord oriental. Evolution climatique et hydrologique depuis le dernier maximum glaciaire. *Mem. Inst. Geol. Bassin Aquitaine*, 17.
- Turon, J.L., and Londeix, L., 1988. Les assemblages de kystes de dinoflagellés en Méditerranée occidentale (Mer d'Alboran): mise en évidence de l'évolution des paléoenvironnements depuis le dernier maximum glaciaire. *Bull. Cent. Explor.-Prod. Elf-Aquitaine*, 12:313–344.
- UNESCO, 1968. *Vegetation map of the Mediterranean region*.
- Vergnaud-Grazzini, C., and Pierre, C., 1991. High fertility in the Alboran Sea since the Last Glacial Maximum. *Paleoceanography*, 6:519–536.
- Versteegh, G.J.M., 1994. Recognition of cyclic and non-cyclic environmental changes in the Mediterranean Pliocene: a palynological approach. *Mar. Micropaleontol.*, 23:147–183.
- Wall, D., Dale, B., Lohmann, G.P., and Smith, W.K., 1977. The environmental and climatic distribution of dinoflagellate cysts in modern marine sediments from regions in the North and South Atlantic Oceans and adjacent seas. *Mar. Micropaleontol.*, 2:121–200.
- Wall, D., and Warren, J.S., 1969. Dinoflagellates in the Red Sea piston cores. In Degens, E.T., and Ross, D.A. (Eds.), *Hot Brines and Recent Heavy Metal Deposits in the Red Sea*: New York (Springer-Verlag), 317–328.
- Walter, W., 1974. *Die Vegetation Ost-Europas, Nord-und Zentralasiens*: Stuttgart (Gustav Fisher).
- Walter, W., Harnickell, E., and Mueller-Dombois, D., 1975. *Climate-Diagram Maps*: Berlin (Springer Verlag).
- Watts, W.A., Allen, J.M.R., Huntley, B., and Fritz, S.C., 1996. Vegetation history and climate of the Last 15,000 years at Laghi di Monticchio, Southern Italy. *Quat. Sci. Rev.*, 15:113–132.
- Wijmstra, T.A., 1969. Palynology of the first 30 meters of a 120-meter deep section in northern Greece. *Acta Botan. Neerland.*, 18:511–528.
- Willis, K.J., 1994. The vegetational history of the Balkans. *Quat. Sci. Rev.*, 13:769–788.
- Zonneveld, K.A.F., 1996. Palaeoclimatic and palaeo-ecologic changes in the Eastern Mediterranean and Arabian Sea regions during the last deglaciation: a palynological approach to land-sea correlation. *LPP Contrib. Ser.*, 3:1–199.

Date of initial receipt: 5 May 1997

Date of acceptance: 16 December 1997

Ms 161SR-238

Appendix

List and Systematics of Identified Dinocysts from Quaternary Sediments of Site 976

The dinoflagellate cysts nomenclature followed herein is that of Lentin & Williams 1993.

Division: Dinoflagellata (Bütschli, 1885) Fensome et al., 1993

Class: Dinophyceae Pascher, 1914

Order: Peridinales Haeckel, 1894

- Ataxiodinium choanum* Reid, 1974
- Achomospaera andalousiensis* Jan du Chêne, 1977 emend. Jan du Chêne & Londeix, 1988
- Achomospaera ramosasimilis* (Yun, 1981) Londeix et al. (in press)
- cysts of *Alexandrium excavatum* (Braarud, 1945) Balech, 1985
- Algidasphaeridium?* cf. *minutum* (Harland & Reid in Harland et al., 1980) Matsuoka & Bujak, 1988. Specimens with morphology close to type material. The modern distribution of height percentages of *A.?* *minutum* is restricted to high latitude surface water (e.g., Mudie, 1992; Rochon, 1997). Because of their unexpected occurrence in Mediterranean Sea, our specimens are designated as *A.?* cf. *minutum* pending further taxonomic investigations.
- Amiculospaera umbracula* Harland, 1979
- Bitectatodinium tepikiense* Wilson, 1973
- Brigantedinium cariacense* (Wall, 1967) Reid, 1977
- Brigantedinium simplex* (Wall, 1965) Reid, 1977
- Dalella chathamense* McMinn & Sun, 1994
- Hystrichokolpoma rigaudiae* Deflandre & Cookson, 1955
- Impagidinium aculeatum* (Wall, 1967) Lentin & Williams, 1981
- Impagidinium japonicum* Matsuoka, 1983b
- Impagidinium pallidum* Bujak, 1984
- Impagidinium paradoxum* (Wall, 1967) Stover & Evitt, 1978
- Impagidinium patulum* (Wall, 1967) Stover & Evitt, 1978
- Impagidinium plicatum* Versteegh & Zevenboom, 1995
- Impagidinium sphaericum* (Wall, 1967) Lentin & Williams, 1981
- Impagidinium striatum* (Wall, 1967) Stover & Evitt, 1978
- Impagidinium velorum* Bujak, 1984
- Lejeunecysta diversiforma* (Bradford, 1977) Artzner & Dörhöfer, 1978
- Lejeunecysta oliva* (Reid, 1977) Turon & Londeix, 1988
- Lejeunecysta sabrina* (Reid, 1977) Bujak, 1984
- Lingulodinium machaerophorum* (Deflandre & Cookson, 1955) Wall, 1967
- Melitasphaeridium aequabile* Matsuoka, 1983b
- Nematosphaeropsis labyrinthea* (Ostenfeld, 1903) Reid, 1974
- Operculodinium centrocarpum* (Deflandre & Cookson, 1955) Wall, 1967. A few specimens have very short processes.
- Operculodinium israelianum* (Rossignol, 1962) Wall, 1967
- Operculodinium janduchenei* Head et al., 1989
- cysts of *Polykrikos schwartzii* Bütschli, 1873
- Polysphaeridium zoharyi* (Rossignol, 1962) Bujak et al., 1980
- cysts of *Pentapharsodinium* cf. *dalei* Indelicato & Loeblich, 1986. Specimens with morphology close to type material. The modern distribution of height percentages of *P. dalei* is restricted to high-latitude surface water (e.g. Mudie, 1992; Rochon, 1997 as *Protoperidinium faeroense*). Because of their unexpected occurrence in Mediterranean Sea, our specimens are designated as *P.* cf. *dalei* pending further taxonomic investigations. Two morphotypes were found.

Pyxidinoopsis? sp.: Some specimens tentatively attributed to the genus *Pyxidinoopsis* Habib, 1975
Pyxidinoopsis reticulata McMinn & Sun, 1994
Quinquecuspis concreta (Reid, 1977) Harland, 1977
Selenopemphix nephroides Benedek, 1972
Selenopemphix quanta (Bradford, 1975) Matsuoka, 1985. Several morphotypes have been found.
Spiniferites belerius Reid, 1974
Spiniferites bentorii (Rossignol; 1964) Wall & Dale, 1970. Several morphotypes were found.
Spiniferites bulloideus (Deflandre & Cookson, 1955) Sarjeant, 1970
Spiniferites delicatus Reid, 1974
Spiniferites elongatus Reid, 1974
Spiniferites granulatus Davey, 1969. Because of their close granular wall ornamentation, *S. pachydermus* and *S. granulatus* have been grouped under *Spiniferites* "granular" gr.
Spiniferites hyperacanthus (Deflandre & Cookson, 1955) Cookson & Eisenack, 1974. Because of their close morphology and ecology, *S. hyperacanthus*

and *S. mirabilis* have been grouped in the text under *S. mirabilis* s.l.
Spiniferites lazus Reid, 1974
Spiniferites membranaceus (Rossignol, 1964) Sarjeant, 1970. Several morphotypes have been found.
Spiniferites mirabilis (Rossignol, 1964) Sarjeant, 1970. Because of their close morphology and ecology, *S. hyperacanthus* and *S. mirabilis* have been grouped in the text under *S. mirabilis* s.l.
Spiniferites pachydermus (Rossignol, 1964) Reid, 1974. Because of their close granular wall ornamentation, *S. pachydermus* and *S. granulatus* have been grouped under *Spiniferites* "granular" grp.
Spiniferites ramosus (Ehrenberg, 1838) & Loeblich, 1966
Spiniferites rubinus (Rossignol; 1964) Sarjeant, 1970
Stelladinium stellatum (Wall & Dale, 1968) Reid, 1977
Tectatodinium pellitum Wall, 1967
Trinovantedinium capitatum Reid, 1977
Tuberculodinium vancampoae (Rossignol, 1962) Wall, 1967
Xandarodinium xanthum Reid, 1977